MAGNETO-OPTICAL PROPERTIES OF Ni, Co, *AND* Fe *IN THE ULTRAVIOLET VISIBLE, AND INFRARED PARTS OF THE SPECTRUM*

G. S. KRINCHIK and V. A. ARTEM'EV

Moscow State University

Submitted July 3, 1967

Zh. Eksp. Teor. Fiz. 53, 1901–1912 (December, 1967)

The polar and equatorial Kerr effects of Ni, Co, and Fe were measured and the $\mathrm{Re}(\epsilon_{xy})$ and $\mathrm{Im}(\epsilon_{xy})$ curves were determined in the 0.22–6.0 eV range. The ultraviolet magneto-optical resonance of Ni was confirmed and similar resonances were observed for Co and Fe. The identical nature of the ϵ_{xy} curves of Ni, Co, and Fe for $h\nu > 1$ eV confirmed Spicer's hypothesis of the indirect nature of the interband transitions in the d-metals. It was found that the magneto-optical method, sensitive to the sign of the spin, made it possible to distinguish the contribution of the right-handed and left-handed spin sub-bands of a ferromagnetic metal to the interband optical transitions.

INTRODUCTION

To determine the nature of the ferromagnetism of the d-metals it is necessary not only to determine their Fermi surfaces but also to solve a more complex problem: to determine completely the energy spectrum of electrons in the outer bands of these metals. Information of this type can be obtained either by x-ray spectroscopy or by various other optical methods: conventional optical spectroscopy, magneto-optics, photoelectric emission.

The range of frequencies which can be investigated by optical methods may be divided arbitrarily into three regions. In the 0.1–1.0 eV region, where the intraband transitions play the main role, the interband transitions begin to appear as well and the absorption edges of the latter have anomalously small values because of the overlap of the s-, p-, and d-bands. In this region the interband optical transitions are direct and consequently, by investigating the anomalies associated with the singularities of the interband density of states, we can - in principle - determine the nature of the energy bands near the Fermi level by measuring the exchange and spin-orbital splitting, etc.[1]

In the 1—4.5 eV region, corresponding to the width of the 3d band, the main effects are associated with the interband transitions. The interpretation of experimental results is complicated by the fact that, as shown by Spicer,[1,2] the high-energy interband transitions, in which the 3d-band electrons participate, are indirect. In this case, the optical methods should give information on the products of the densities of states in the filled and vacant parts of the band, which - after some simplifying assumptions - can be used to determine the density of states of the filled part of the 3d-band.[2]

In the ultraviolet part of the spectrum (4.5–6 eV), the magneto-optical[3] and the optical[4] methods in the case of Ni, and the photoelectric emission method in the case of Ni, Fe, and Co[5] have indicated resonances which correspond to strong density-of-states maxima 5 eV below the Fermi level. The presence of these maxima is difficult to explain on the basis of one-electron representations of the 3d-band structure of Ni and Fe. Phillips[6] and Mott ([1], p. 314) have assumed that in noble and in d-metals these ultraviolet resonances are due to many-electron excitations of the exciton type. Spicer[5] has concluded - on the basis of the absence of a similar resonance in Pd - that it is basically due to the ferromagnetism of Ni, Co, and Fe.

The purpose of the present investigation was to study the frequency dependence of the real and imaginary parts of the nondiagonal component of the permittivity tensor ϵ_{xy} of Ni, Co, and Fe in the 0.2–6.0 eV range, which covers all the three energy regions discussed above. Although the magneto-optical method should, generally speaking, give the same results as the photoelectric emission and optical spectroscopy methods, it has an advantage over the latter methods because, in contrast to ϵ_{xx}, ϵ_{xy} changes its sign when the spin orientation is reversed. Therefore, using the magneto-optical method we can distinguish the influence of the right-handed and left-handed spin sub-bands.

MEASUREMENT METHOD

A block diagram of the apparatus used in the measurements of the polar Kerr effect (α_K) by a dynamic method is shown in Fig. 1. An alternating magnetic field (f = 70 cps) of 6600 Oe amplitude was established in a 6 mm wide gap of an electromagnet. The electromagnet was supplied from a low-frequency 300 W amplifier and the magnet winding was connected in series with a capacitor to compensate for the reactance

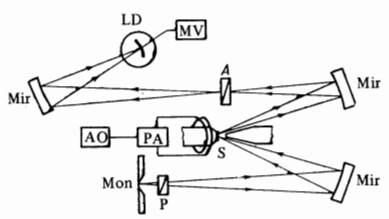

FIG. 1. Block diagram of the apparatus used in the measurement of the polar Kerr effect by a dynamic method: Mon—exit slit of a monochromator; P—a polarizer; A—an analyzer; Mir—mirrors; S—a sample; LD—a light detector; MV—a microvoltmeter; AO—an audio-frequency oscillator; PA—a power amplifier.

of the winding. To suppress stray signals a light detector was placed at a distance of 5 m from the electromagnet. The angle of incidence of light on a sample was governed by the shape of the sharp pole-piece of the electromagnet and it amounted to 15–20°. The sample, glued to the flat electromagnet pole-piece, was subjected to magnetization reversals at a frequency of f = 70 cps; this modulated the angle of rotation of the plane of polarization of light reflected by the sample and the intensity of light passing through an analyzer. A polarizer was tuned to the p- or s-wave and the analyzer was turned through an angle of 45° with respect to the polarizer. The values of α_K for the normal incidence of light were found from arithmetic means of α_K^p and α_K^s. FÉU-39A and FÉU-79 photomultipliers, a cooled PbS photoresistor, or a cooled InSb photodiode were used as detectors of light of various wavelengths. An alternating signal from the load of the light detector was applied to the input of a V6-2 microvoltmeter. In some cases an SD-1 synchronous detector was also used. The measurements were carried out using a DMR-4 monochromator in the 5.9–0.5 eV range and an IKM-1 infrared monochromator in the 0.5–0.225 eV range. The angular aperture of the light beam incident on the sample was not more than 40′ when the DMR-4 is used and not more than 1° when the IKM-1 was used. The equatorial effect was also measured by a dynamic method using similar apparatus for which a block diagram had been given in [7]. In the latter case we used a smaller electromagnet, which produced a field of 1500 Oe, sufficient for the saturation magnetization of the samples parallel to their surface.

Ni, Co, and Fe samples were plates of 0.3 × 16 × 24 mm dimensions. The polar and equatorial Kerr effects were measured on the same samples. The purity of these samples was 99.99%. They were subjected to mechanical polishing, annealing, and electrolytic polishing before measurements.

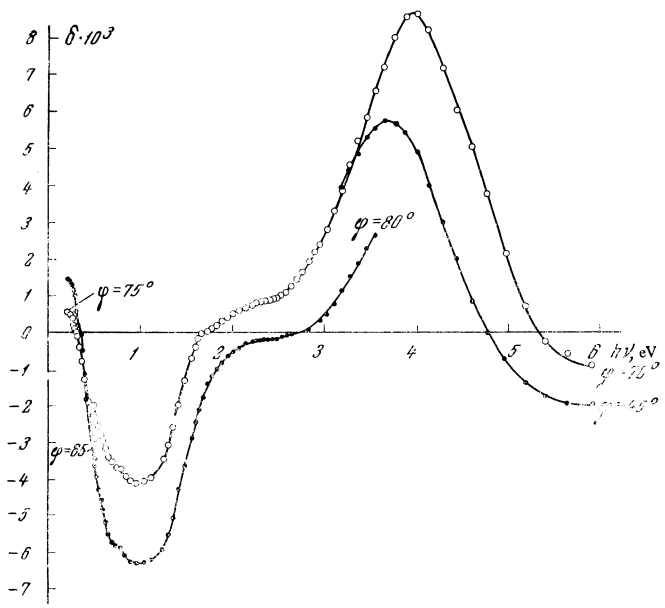

FIG. 2. Equatorial Kerr effect of Ni for two angles of incidence of light.

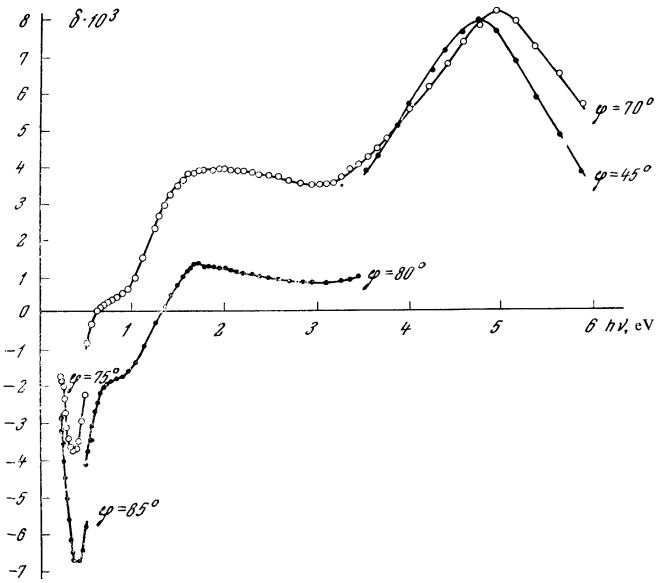

FIG. 3. Equatorial Kerr effect of Co for two angles of incidence of light.

EQUATORIAL KERR EFFECT

Figures 2–4 give the experimental curves of the equatorial Kerr effect δ of Ni, Co, and Fe for two angles of incidence of light φ_1 and φ_2. From these values of $\delta\varphi_1$ and $\delta\varphi_2$, we calculated ϵ_1' and ϵ_2' using the formula [7]

$$\delta = a\varepsilon_1' + b\varepsilon_2', \tag{1}$$

where $\epsilon_{xx} = \epsilon_{yy} = \epsilon_1 - i\epsilon_2$, $\epsilon_{xy} = -\epsilon_{yx} = i\epsilon'$, $\epsilon' = \epsilon_1' - i\epsilon_2'$. The angles φ_1 and φ_2 were selected so that the coefficients $a(\varphi_1)$, $b(\varphi_1)$ and $a(\varphi_2)$, $b(\varphi_2)$ were linearly independent. Because of the rapid rise of ϵ_1 and ϵ_2 in the infrared region, this condition was difficult to satisfy even at the maximum values of φ_1 and φ_2; this was the main source of systematic error in the determination of ϵ_1' and ϵ_2'. Moreover, when φ was increased, the systematic error in the measure-

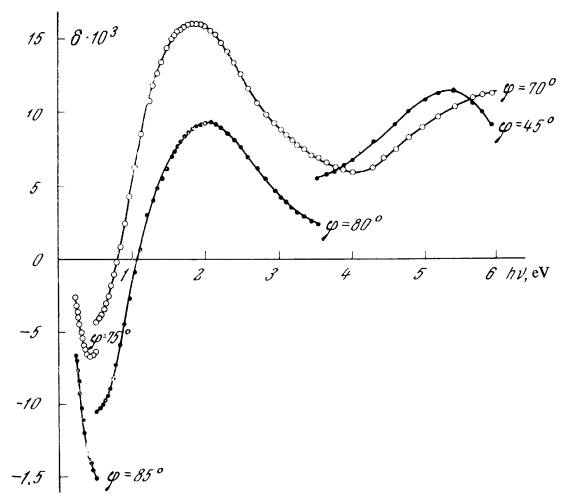

FIG. 4. Equatorial Kerr effect of Fe for two angles of incidence of light.

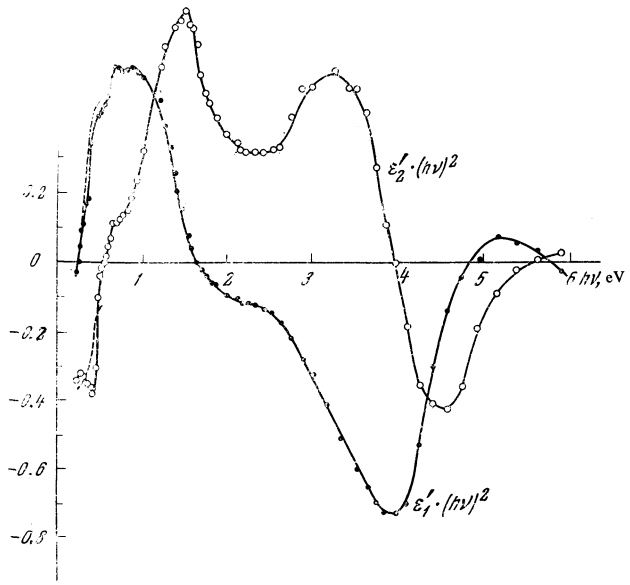

FIG. 5. Curves showing ϵ_1' and ϵ_2' of Ni, calculated from the experimental values of δ_{φ_1} and δ_{φ_2} (Fig. 2). The dashed parts of the curves were calculated from the values of δ for $\varphi = 75°$ and from α_K (Fig. 8).

ment of δ increased because of the uneven surfaces of the samples, the influence of scattered light, etc.

Figures 5–7 show the calculated curves $\epsilon_1'(h\nu)^2$ and $\epsilon_2'(h\nu)^2$ ($h\nu$ is in eV). The values of ϵ_1 and ϵ_2 were taken from [8] (cf. also references in [7,9]). The ϵ_1 and ϵ_2 curves were smoothed out at the points where the values of the optical constants, taken from different papers, were matched; in the ultraviolet region, the values of ϵ_1 and ϵ_2 for $\lambda < 0.24\ \mu$, were found by extrapolation. The discontinuities in the ϵ_1' curves of Fe (Fig. 7) and Ni (Fig. 5) and the corresponding discontinuity in the α_K^{calc} curve of Co (Fig. 8) at $h\nu = 0.5$ eV are due to a transition from $\varphi_1 = 70°$ and $\varphi_2 = 80°$ to $\varphi_1 = 75°$ and $\varphi_2 = 85°$.

The values of ϵ_1' and ϵ_2' in Figs. 5–7 were multiplied by $(h\nu)^2$ in order to, firstly, equalize the maxima of the curves in the infrared, visible, and ultraviolet parts of the spectrum. Secondly, the theoretical formulas obtained on the assumption of a direct interband mechanism [10] were in the form $p/(h\nu)^2$. The most interesting was the frequency dependence of the quantity p, which was proportional to the interband density of states and to the characteristic magneto-optical parameter Q. Therefore, our representation of these curves is the most appropriate from the physical point of view, although there are no corresponding calculations of the magneto-optical effects for indirect transitions.

POLAR KERR EFFECT

The polar Kerr effect α_K of Ni, Fe, and Co was measured to enable us to use a comparison of the experimental and calculated values of α_K to check, at least qualitatively, the degree of reliability of the determination of ϵ_1' and ϵ_2' from the equatorial Kerr effect.

Figure 8 gives the α_K^{exp} and α_K^{calc} curves, where the values of α_K^{calc} were found from the formula

$$\alpha_K = a_K\varepsilon_1' + b_1\varepsilon_2', \tag{2}$$

where

$$a_1 = \frac{-k(3n^2-k^2-1)}{(n^2+k^2)[(n^2-k^2-1)^2+4n^2k^2]}$$

$$b_1 = \frac{n(n^2-3k^2-1)}{(n^2+k^2)[(n^2-k^2-1)^2+4n^2k^2]},$$

using ϵ_1' and ϵ_2' from Figs. 5–7 and previous values of the optical constants. Because of additional light losses in the apparatus, the values of α_K could be measured only up to $\lambda = 0.28\ \mu$. The values of α_K for Fe and Co, corresponding to the magnetic saturation, were found by linear extrapolation of the experimental values of α_K (H = 6600 Oe) to $\mathbf{H} = 4\pi\mathbf{I}_S$.

Comparison of the experimental and calculated polar Kerr effect curves showed that, although the absolute

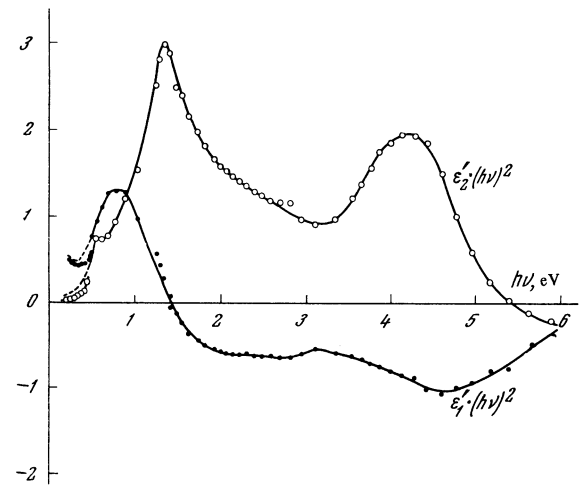

FIG. 6. Curves showing ϵ_1' and ϵ_2' for Co, calculated from the experimental values of δ_{φ_1} and δ_{φ_2} (Fig. 3). The dashed parts of the curves were calculated from the values of δ for $\varphi = 75°$ (Fig. 3) and from α_K (Fig. 8).

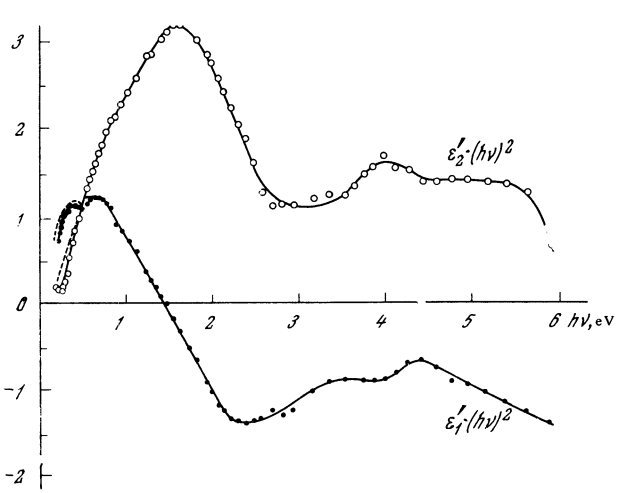

FIG. 7. Curves showing ϵ_1' and ϵ_2' for Fe, calculated from the experimental values of δ_{φ_1} and δ_{φ_2} (Fig. 4). The dashed parts of the curves were calculated from the values of δ for $\varphi = 75°$ (Fig. 4) and from α_K (Fig. 8).

values of α_K^{exp} and α_K^{calc} differed sometimes by a factor of 1.5–2 (the nickel sample was probably not magnetized to saturation in a field of 6600 Oe), the general nature of the frequency dependence of α_K was described quite satisfactorily. In particular, the regions where α_K changed sign coincided and the characteristic dip of α_K of Ni and Co in the visible range was reproduced. Therefore, we could assume that the principal features of the frequency dependences of ϵ_1' and ϵ_2' in Figs. 5–7 were represented correctly. The quantitative differences between α_K^{calc} and α_K^{exp} in the near infrared, visible, and ultraviolet regions were evidently due to the fact that the optical constants were not determined using the samples employed in the magneto-optical measurements. Since, as shown in the preceding section, the dominant error in the far infrared region was associated with the linear dependences of the coefficients of ϵ_1' and ϵ_2' in the polar effect (δ) equations for $\varphi = 75°$ and $\varphi = 85°$, we plotted the ϵ_1' and ϵ_2' curves for $h\nu < 0.5$ eV (Figs. 5–7) calculated from the equations for the equatorial and polar effects:

$$\delta(\varphi = 75°) = f(\varepsilon_1', \varepsilon_2'), \quad \alpha_K = f(\varepsilon_1', \varepsilon_2').$$

In view of the large error in the determination of ϵ_1' and ϵ_2' in the infrared region, we compared our results with those reported for Ni, Co, and Fe by other authors.[10,11] Our values of ϵ_1' and ϵ_2' for Ni in the 0.22–1.8 eV range were in fairly good agreement with the earlier determinations of ϵ_1' and ϵ_2' from the equatorial Kerr effect[7,9] but they differed considerably from the values reported in[10,11]. The same was found for the results for Fe and Co in the 0.5–1.6 eV range when they were compared (cf. Figs. 6 and 7) with our earlier results[9] and with the results of Afanas'eva et al.[11]

To check the results of Martin et al.[10] and Afanas'eva et al.[11] we employed the approach already described, i.e., we used the values of ϵ_1', and ϵ_2', found from the two magneto-optical effects, to determine the third effect and we compared the calculated values with the experimental ones. The α_K curve in the 0.22–1.5 eV region determined in this way from the results of Martin et al.[10] was in complete disagreement with the experimental data. A change of sign at $h\nu \approx 0.9$ eV (cf. Fig. 5) was absent from the calculated curve and the effect reached a value $+8 \times 10^{-3}$ rad in this region. A change of sign at $h\nu \approx 0.3$ eV and a value of -8×10^{-3} rad at $h\nu \approx 0.22$ eV were predicted while the experimental values of α_K in this region were positive and approximately equal to $+2 \times 10^{-3}$ rad (cf. Fig. 5). Obviously, the incorrect values of ϵ_1' and ϵ_2' reported in[10] were due to an underestimation of the experimental values of $\delta(\varphi = 85°)$ obtained in that investigation [cf. the corresponding $\delta(\varphi = 85°)$ curves in Fig. 2 and in[7]/].

A strong disagreement with the experimental values (cf. table) was observed also when the $\delta(\varphi = 75°)$, $\delta(\varphi = 80°)$ and $\delta(\varphi = 85°)$ curves of Ni, Fe, and Co were calculated using the values of ϵ_1' and ϵ_2' given in[11]. The absolute values of ϵ_1' and ϵ_2' reported in[11] were very large and the ratios $|\epsilon_2'|/|\epsilon_2|$ and $|\epsilon_1'|/|\epsilon_1|$ reached the unlikely values of 40–70%. Since the α_K curves reported in[11] were in quite good agreement with the curves shown in Fig. 8, it was obvious that the cause of the incorrect determination of ϵ_1' and ϵ_2' in[11] was a systematic error in the measurement of the difference $\alpha_K^p - \alpha_K^s$ at $\varphi = 30°$, which was used as the second equation in the determination of ϵ_1' and ϵ_2'.

$h\nu$, eV	Ni		Fe		Co	
	$\delta^{calc} \cdot 10^3$	$\delta^{exp} \cdot 10^3$	$\delta^{calc} \cdot 10^3$	$\delta^{exp} \cdot 10^3$	$\delta^{calc} \cdot 10^3$	$\delta^{exp} \cdot 10^3$
			$\varphi = 80°$			
1.240	—50.20	—5.95	45.00	3.03	14.85	—0.3
1.034	—45.52	—6.29	— 4.70	— 0.82	—65.90	—1.35
0.827	—41.62	—6.12	—62.70	— 5.91	—59.00	—1.8
0.620	—32.38	—5.19	—94.00	—10.10	—69.40	—2.45
0.517	—21.86	—3.91	—95.20	—10.40	—80.90	—3.55
			$\varphi = 85°$			
0.451	—13.85	—2.57	—114	—14.5	—109	—6.46
0.355	— 6.55	—0.48	— 90.6	—12.8	— 91.6	—6.42
0.31	— 4.07	0.22	— 92	—11.2	— 69.0	—5.63
0.248	— 1.78	1.35	— 35.3	— 7.52	— 40.7	—3.52

DISCUSSION OF RESULTS

The main result of the present investigation is a reliable frequency dependence of ϵ' of Ni, Co, and Fe in the infrared, visible, and ultraviolet frequency parts of the spectrum. An interpretation of the magneto-optical spectra of the ferromagnetic d-metals, shown in Figs. 5–7, cannot yet be given because of the absence of a self-consistent theory of electron states of metals lying well below the Fermi level. Therefore, we shall compare the results obtained for Ni, Co, and Fe by various optical methods using the existing qualitative representations of the electron structure of transition metals and of the nature of interband optical transitions.

Examination of the ϵ_1' and ϵ_2' curves of Ni, Co, and Fe shows clearly that their frequency dependences are identical in the region $h\nu > 1$ eV, although the crystal structures of these metals are different. Since the density-of-states curves of the 3d-band of Ni, Co, and

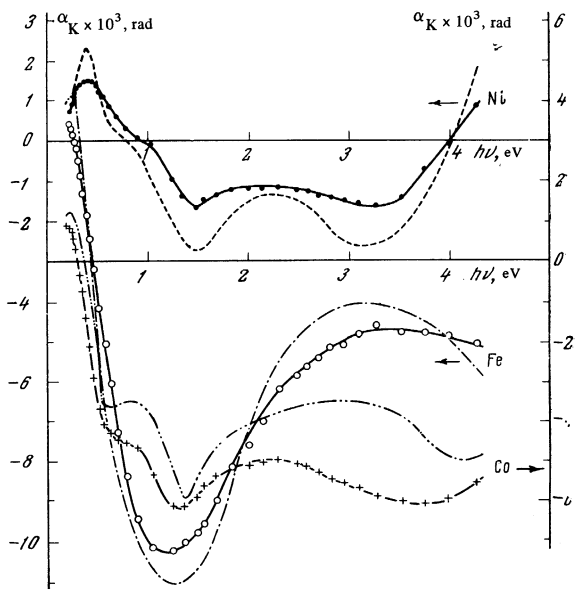

FIG. 8. Polar Kerr effect curves α_K^{exp} and curves (shown dashed) calculated from ϵ_1' and ϵ_2' (Figs. 5–7).

Fe, determined by the photoelectric emission method method,[5] are also of identical shape, we shall regard the results obtained as a confirmation of Spicer's conclusion[1,2] that the indirect interband optical transitions are dominant in transition metals at $h\nu \gtrsim 1$ eV.

Curves shown in Figs. 2–7 indicate that Co and Fe exhibit an ultraviolet magneto-optical resonance, which has been first reported for Ni in[3]. If we determine the frequency of this resonance, $h\nu_0$, from the maximum of $|\epsilon_2'|$, we then find (Fig. 5) that this frequency correspond to 4.6 eV for Ni. This value is practically identical with the value of $h\nu_0$ determined earlier by the magneto-optical method[3] and is in good agreement with the values obtained later by optical[4] and photoemission[1] methods. In the case of Co and Fe there is no such $|\epsilon_2'|$ maximum in the investigated range of frequencies, but the nature of the ultraviolet parts of the δ curves in Figs. 2–4 shows that Co and Fe exhibit a similar ultraviolet magneto-optical resonance at higher frequencies. If we estimate these frequencies from the shift of the zero value of ϵ_2' of Co and Fe with respect to Ni, we find from Figs. 5–7 that $h\nu_0 \approx 6.0$ eV for Co and $h\nu_0 \approx 6.6$ eV for Fe. These values are in good agreement with the results obtained for Co and Fe by the photoelectric emission method.[5]

According to[5], the ultraviolet density-of-states maxima of the 3d-bands of Co and Fe lie about 5.2 and 5.8 eV below the Fermi level. Since the half-width of the unfilled part of the 3d-band of Co and Fe is larger than that of Ni and since it is of the order of 0.5 eV, the values of $h\nu_0$ given above are in quantitative agreement with the energies of electron transitions from the ultraviolet maximum to the unfilled part of the 3d-band. Similar fundamental frequencies should be observed in the optical spectra of Co and Fe but, unfortunately, no reliable measurements of ϵ_1 and ϵ_2 have yet been carried out for these metals in the ultraviolet part of the spectrum.

In the 1–4.5 eV range the ϵ_2' curves of Ni, Co, and Fe have a characteristic two-hump shape. The simplest explanation of this observation would be that the ϵ_2' spectra reflect the two-hump nature of the density-of-states curve of the filled part of the 3d-band, but this explanation does not agree with the results of a determination of the density of states in the 3d-band by the electron photoemission method. The point is that the density-of-states curves of the 3d-bands of Ni, Fe, and Co given in[5] have only one maximum in the visible part of the spectrum, located about 2.3 eV below the Fermi level.

The magneto-optical and photoemission results can be made to agree by assuming that the curve representing the positive values of ϵ_2', corresponding to electron transitions in the 3d↓ sub-band (spins antiparallel to I_S), is "suppressed" by the ϵ_2' curve of opposite sign, corresponding to transitions in the 3d↑ sub-band (spins parallel to I_S). Both curves should have maxima in the 2–3 eV region, which represent transitions from the density-of-states maximum at 2.3 eV to the unfilled parts of the 3d-bands, but the contribution of the 3d↑ transitions is less because of the narrower unfilled part of the 3d↑ sub-band. The optical data on Ni do not contradict this assumption because the experimental $\epsilon_2(h\nu)^2$ curve given in[4] has, in addition to a maximum corresponding to the ultraviolet resonance at 4.6 eV, a further maximum in the 1.5–2.5 eV region, which can be attributed to the combined effect of transitions in the 3d↓ and 3d↑ sub-bands.

We attempted to obtain the form of the $\epsilon_2' = \epsilon_2'\downarrow - \epsilon_2'\uparrow$ curve using the simplest formula for the mechanism of indirect transitions:

$$\varepsilon_2' = \frac{Q}{(h\nu)^2} \int_{E_p}^{E_p - h\nu} \eta_{\text{vac}}(E)\,\eta_{\text{fil}}(E - h\nu)\,dE, \qquad (3)$$

where η_{vac} and η_{fil} are the corresponding densities of states; Q is a magneto-optical parameter which is assumed to be constant for all the interband transitions. Using this formula, we calculated the contributions of the right-handed and left-handed spin sub-bands and then we found the difference and sum of these contributions (in relative units), corresponding to the magneto-optical and optical spectra of indirect interband transitions. It was possible to obtain two-hump ϵ_2' curves with a characteristic dip described earlier if it was assumed that the transition from the paramagnetic to the ferromagnetic state not only produced a relative shift of the right-handed and left-handed spin sub-bands but also altered the shape of the density-of-states curves, for example, by altering the relative positions of the density-of-states maxima in the 3d↑ and 3d↓ sub-bands (the maximum of the density in the 3d↑ sub-band shifted in the direction of the bottom of the band). The $\epsilon_2'(h\nu)^2$ and $\epsilon_2(h\nu)^2$ curves obtained in this way are shown in Fig. 9. We note that Spicer has reconstructed the density of states in the 3d-band[1] without distinguishing transitions in the right-handed and left-handed spin sub-bands and, consequently, he has not allowed for the difference between the widths of the unfilled parts of the 3d↑ and 3d↓ sub-bands; this may distort the results for ferromagnetic d-metals quite considerably.

The agreement with other methods is more difficult to obtain in the infrared parts of the ϵ_1' and ϵ_2' curves. In this case the transition energy is comparable with

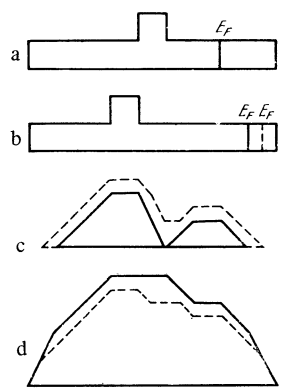

FIG. 9. Curves showing ϵ_1' and ϵ_2' as a function of $h\nu$, calculated from Eq. (2) for a model with one density-of-states maximum in the filled part of the 3d-band and an arbitrary value of the parameter Q = const: a) density of states in the 3d↓ sub-band; b) density of states in the 3d↑ sub-band; c) $\epsilon_2'(h\nu)^2 = (\epsilon_2'\downarrow - \epsilon_2'\uparrow)(h\nu)^2$; d) $\epsilon_2(h\nu)^2 = (\epsilon_2\downarrow + \epsilon_2\uparrow)(h\nu)^2$. The dashed curves and lines represent the Fermi level position in the 3d↑ sub-band.

the widths of the unfilled parts of the 3d-band and, therefore, the spectra obtained by the magneto-optical method, which is sensitive to the sign of the band, may differ considerably. Moreover, the intraband transitions may make a considerable contribution to ϵ_1' and ϵ_2' in this part of the spectrum. In particular, the negative sign of ϵ_1' and ϵ_2' for Ni and the positive sign for Fe and Co in the $h\nu \approx 0.2$–0.3 eV range is evidently associated with the sign of the static ferromagnetic Hall effect. As far as the interband effects are concerned, the magneto-optical spectra of Fe in the $h\nu < 1$ eV range have no definite singularities associated with the interband transition singularities. The δ, ϵ_1', and ϵ_2', and α_K of Co curves all exhibit a strong anomaly in the 0.65–0.7 eV range. Singularities in the ϵ_1' and ϵ_2' curves, which are in qualitative agreement with the anomalies observed earlier,[1,7] are observed also in the infrared spectrum of Ni.

These singularities have been discussed in detail in[1,12-14] and they have been used in the development of various models of the electronic structure of ferromagnetic Ni near the Fermi level. However, it has not yet been possible to establish an unambiguous and reliable quantitative agreement between the magneto-optical data and any particular electron structure model. Therefore, further progress can be made only by obtaining additional experimental information in the far infrared region, by observing the behavior of these singularities in alloys, by studying their temperature dependences, etc. In this respect it would be most interesting to study the long-wavelength edge of the interband transitions in the $3d^{\uparrow}$ and $3d^{\downarrow}$ sub-bands of a ferromagnetic metal.

The authors are very grateful to B. M. Glukhovskiĭ and A. V. Kulymanov for the supply of an FÉU-79 photomultiplier and a low-noise InSb photodiode.

[1] Optical Properties and Electronic Structure of Metals and Alloys (ed. F. Abeles), Amsterdam, 1966.
[2] W. E. Spicer, Phys. Rev., 154, 385 (1967).
[3] G. S. Krinchik and A. A. Gorbachev, FMM, 11, 203 (1961).
[4] H. Ehrenreich, H. R. Phillipp, and D. J. Olechna, Phys. Rev. 131, 2469 (1963).
[5] A. Y.-C. Yu and W. E. Spicer, Phys. Rev. Letters 17, 1171 (1966).
[6] J. C. Phillips, Phys. Rev. 140, A1254 (1965).
[7] G. S. Krinchik and G. M. Nurmukhamedov, Zh. Eksp. Teor. Fiz. 48, 34 (1965) [Sov. Phys.-JETP, 21, 22 (1965)].
[8] Landolt-Börnstein, Physikalisch-Chemische Tabellen, Berlin, 1923.
[9] G. S. Krinchik, Izv. AN SSSR, seriya fiz. 28, 481 (1964).
[10] D. H. Martin, K. F. Neal, and T. J. Dean, Proc. Phys. Soc. (London) 86, 605 (1965).
[11] L. A. Afanas'eva, G. A. Bolotin, and M. M. Noskov, FMM 22, 828 (1966); L. A. Afanas'eva and M. M. Kirillova, FMM, 23, 472 (1967).
[12] B. R. Cooper, Phys. Rev. 139, A1504 (1965).
[13] G. S. Krinchik and E. A. Ganshina, Phys. Letters 23, 294 (1966).
[14] L. Hodges, H. Ehrenreich, and N. D. Lang, Phys. Rev. 152, 505 (1966).

Translated by A. Tybulewicz
217